ACS OMEGA

http://pubs.acs.org/journal/acsodf

Article

Water Content-Controlled Formation and Transformation of Concomitant Pseudopolymorph Coordination Polymers

Behrouz Notash,* Mona Farhadi Rodbari, and Maciej Kubicki

Cite This: *ACS Omega* 2023, 8, 13140−13152

Read Online

ACCESS | Metrics & More | Article Recommendations | Supporting Information

ABSTRACT: Two concomitant pseudopolymorph coordination polymers $\{[Cd_2L_2(OAc)_4]\cdot 2DMSO\}_n$ (**1**) and $\{[CdL(OAc)_2]\cdot 2.75H_2O\}_n$ (**2**) were synthesized by self-assembly of 1,4-bis(4-pyridyl)-2,3-diaza-1,3-butadiene (**L**) and cadmium acetate in DMSO. Single-crystal X-ray diffraction confirmed that 1D ladder structural motifs exist for pseudopolymorphs **1** and **2** which contain DMSO and water guest molecules, respectively. Our study illustrated the active role of solvent water content in obtaining compound **2**. We find that the presence of water as an impurity in the DMSO solvent creates the possibility of formation of concomitant pseudopolymorph coordination polymers which is a unique event. Furthermore, our analyses showed the effect of environmental humidity on the transformation of unstable compound **1**. 1D ladder pseudopolymorphic compound **1** could be transformed to guest-free 1D linear compound $[CdL(OAc)_2(H_2O)]_n$ (**3′**) (the powder form of single crystals of **3**) through a scarce case of water absorption from air. Also, the crystalline material of coordination polymer **3** was transformed to coordination polymer **2** through the dissolution−recrystallization structural transformation process in DMF or DMSO. Our study clarified that the amount of water in the reaction container can control the formation of one of the compounds **2** or **3**. In the presence of a significant amount of water, compound **3** (coordinated water) will be produced, whereas if a small amount of water is present, compound **2** (uncoordinated water) is prepared as an exclusive product.

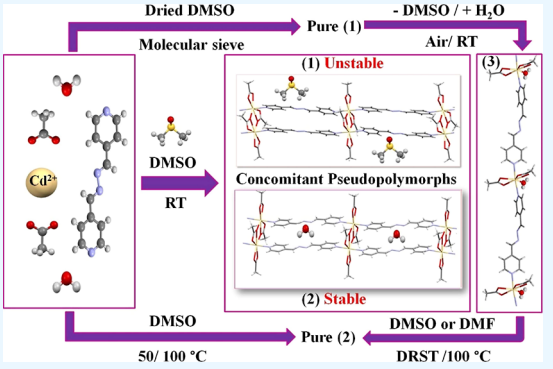

1. INTRODUCTION

The high potential of coordination polymers (CPs),[1] such as magnetic properties,[2,3] catalytic activity,[4,5] gas storage and separation,[6,7] electrical conductivity,[8,9] and sensing,[10,11] has encouraged chemists and crystal engineers to investigate them for more than 20 years.[1] CPs are able to expand in one, two, or three dimensions due to a wide variety of factors that can affect their structure such as ligand(s), metal center(s), anion(s), and solvent(s).[1] One-dimensional (1D) CPs form a wide range of structures such as ladder, linear, helical, zigzag, rotaxane, and ribbon.[12,13]

Solvent system alongside other factors[14−16] plays an important role in tuning the final structure in CPs because it accepts different roles during the self-assembly process such as template, ligand, guest, and both ligand and guest.[17−20] Solvent not only is able to change the final structure but also could affect the crystal's habit and properties by changing the dimension and topology,[21,22] morphology,[16,23] formation of supramolecular isomers,[24,25] conformation of the ligand,[26−28] coordination environment of the metal center,[29] and pore size of the structure.[30,31] Among solvents, water plays a significant role due to it being the most abundant and nontoxic/green solvent. As a result, it has drawn attention through scientific history. Water can be used not only as a green solvent in chemical processes but also can be absorbed from air and take part in the chemical reactions or even interact with the metal center in the self-assembly process.[32−36] In addition, the special ability of water in forming hydrogen bonds enables this solvent to form more stable crystalline CPs.[37] Another area that the solvent can play an important role is supramolecular isomerism.[24,25] Supramolecular isomers are compounds with different supramolecular networks, structure, or topology while the same chemical compositions are used during the self-assembly process.[38,39] Pseudopolymorphs or solvatomorphs are important classes of supramolecular compounds that can differ in the number or type of guest solvent(s) in the structure.[38−43]

Sometimes during the self-assembly process, two or more different kinds of compounds are formed and crystallize together in a special time or reaction condition. Although this event is rather rare, there are some reports about it. In a few interesting cases, supramolecular isomers were formed in the

Received: January 19, 2023
Accepted: March 7, 2023
Published: March 27, 2023

Table 1. Crystallographic and Structure Refinement Data for 1−3

	1	2	2sq	3
empirical formula	$C_{36}H_{44}Cd_2N_8O_{10}S_2$	$C_{16}H_{16}CdN_4O_{6.75}$	$C_{16}H_{16}CdN_4O_4$ (+solvent)	$C_{16}H_{18}CdN_4O_5$
fw/g mol^{-1}	1037.73	484.73	440.73	458.75
crystal color, habit	yellow, needle	yellow, plate	yellow, plate	yellow, polyhedral
temperature/K	298(2)	100	100	298(2)
wavelength λ/Å	0.71073	0.71073	0.71073	0.71073
crystal system	triclinic	monoclinic	monoclinic	orthorhombic
space group	$P\bar{1}$	$I2/a$	$I2/a$	$Pnna$
crystal size/mm	0.50 × 0.30 × 0.20	0.25 × 0.25 × 0.35	0.25 × 0.25×0.35	0.30 × 0.25 × 0.25
a/Å	9.1808(18)	14.6056(4)	14.6056(4)	8.4253(17)
b/Å	12.351(3)	11.9674(4)	11.9674(4)	13.491(3)
c/Å	20.521(4)	23.3975(7)	23.3975(7)	16.459(3)
α/°	87.65(3)	90	90	90
β/°	77.55(3)	99.919(3)	99.919(3)	90
γ/°	86.00(3)	90	90	90
volume/Å^3	2265.9(9)	4028.5(2)	4028.5(2)	1870.8(7)
Z	2	8	8	4
d_{calcd}/g cm^{-3}	1.521	1.599	1.453	1.629
θ range/deg	2.28−25.00	3.5−28.4	3.5−28.4	1.95−25.00
F(000)	1048	1936	1760	920
abs coeff/mm^{-1}	1.090	1.126	1.109	1.201
index ranges	$-10 \le h \le 10$	$-18 \le h \le 19$	$-18 \le h \le 19$	$-10 \le h \le 8$
	$-14 \le k \le 14$	$-14 \le k \le 15$	$-14 \le k \le 15$	$-14 \le k \le 16$
	$-24 \le l \le 24$	$-29 \le l \le 28$	$-29 \le l \le 28$	$-17 \le l \le 19$
collected data	16651	16025	16025	5244
unique data (R_{int})	7948 (0.1399)	4443 (0.032)	4443 (0.032)	1645 (0.0591)
parameter, restrains	513, 0	288, 0	228, 0	111, 0
R_1[a], wR_2[b] [$I > 2\sigma(I)$]	0.0801, 0.2077	0.0303, 0.0718	0.0271, 0.0669	0.0410, 0.0921
GOF on F^2 (S)	0.929	1.09	1.33	1.055
largest diff peak, hole/e Å^{-3}	1.726, −2.390	0.60, −0.67	0.52, −0.68	0.710, −0.601
CCDC no.	2211160	2211161	2211162	2211163

[a] $R_1 = \Sigma||F_o| - |F_o||/\Sigma|F_o|$. [b] $wR_2 = [\Sigma(w(F_o^2 - F_c^2)^2)/\Sigma W(F_o^2)^2]^{1/2}$.

reaction vessel concomitantly.[44−47] Although structural transformation of CPs in the solid phase is highly regarded,[48−56] there are few studies on the structural transformation in the liquid phase in CPs, especially through dissolution−recrystallization structural transformation (DRST).[23,28,36,57−60]

Herein, we report the synthesis and crystal structure of two concomitant pseudo polymorphic CPs **1** and **2** through the self-assembly process in dimethyl sulfoxide (DMSO) by using the ditopic nitrogen donor ligand (**L**) and cadmium acetate. Our results showed that the 1D ladder motifs of **1** and **2** contain free DMSO and water molecules, respectively. In addition, we described the important role of water in the formation/stability of compound **2** and the possibility of formation of concomitant pseudopolymorphs **1** and **2**. Also, water absorption from air facilitates the single crystal-to-powder transformation of 1D ladder in **1** to linear chain in **3′**. A similar transformation was reported in our previous work.[28] Another transformation in this work was conversion from compound **3** (1D linear chain with coordinated water) to compound **2** (1D ladder with guest water) in DMSO or dimethylformamide (DMF) through the DRST process.

2. EXPERIMENTAL SECTION

2.1. Materials and Instruments. 1,4-Bis(4-pyridyl)-2,3-diaza-1,3-butadiene (**L**) was prepared according to the condensation reported method.[61] Compound **3** (crystalline form of **3′**) was synthesized according to previously reported methods.[28] Reagents and organic solvents were purchased from chemical sources and were used without purification. In some experiments, DMSO was dehydrated by an activated molecular sieve. FTIR spectra of the solid compounds were taken as 1% dispersion in KBr using a MB102 Bomem instrument. Uncorrected melting points were obtained by an Electrothermal 9100 instrument. PXRD analysis was performed using a STADIP STOE diffractometer. SEM images were taken by the VEGA3 model of the TESCAN company. A USA DUPONT 951 instrument was used for the thermogravimetric analysis (TGA) of compounds **1** and **2**.

Caution! Cadmium salts and compounds are toxic and should be handled with care.

2.2. Synthesis of $\{[Cd_2L_2(OAc)_4]\cdot 2DMSO\}_n$ (1) and $\{[CdL(OAc)_2]\cdot 2.75H_2O\}_n$ (2). 0.0380 g (0.1426 mmol) of $Cd(OAc)_2.2H_2O$ and 0.030 g (0.1427 mmol) of **L** were dissolved in 2.5 mL of DMSO separately. Then, the solution containing **L** was added to the solution of cadmium salt and stirred in an ambient temperature for 30 min. Then, the slow evaporation method was used for growing single crystals of compound **1**. After 3 days, yellow needle-shaped single crystals of compound **1** were formed. Interestingly, different yellow plate-shaped single crystals of compound **2** were obtained in the vial after 1 week. Compounds **1** and **2** were extracted and separated from each other by a thin needle, and then they were washed with DMSO and *n*-hexane. It should be noted that single crystals of compound **1** were mechanically unstable and become opaque after extracting from the mother solvent. In contrast, single crystals of compound **2** remained stable for

https://doi.org/10.1021/acsomega.3c00405
ACS Omega 2023, 8, 13140−13152

Scheme 1. Concomitant and Pure Synthesis Routes of Compounds 1−3 and 3′[28]

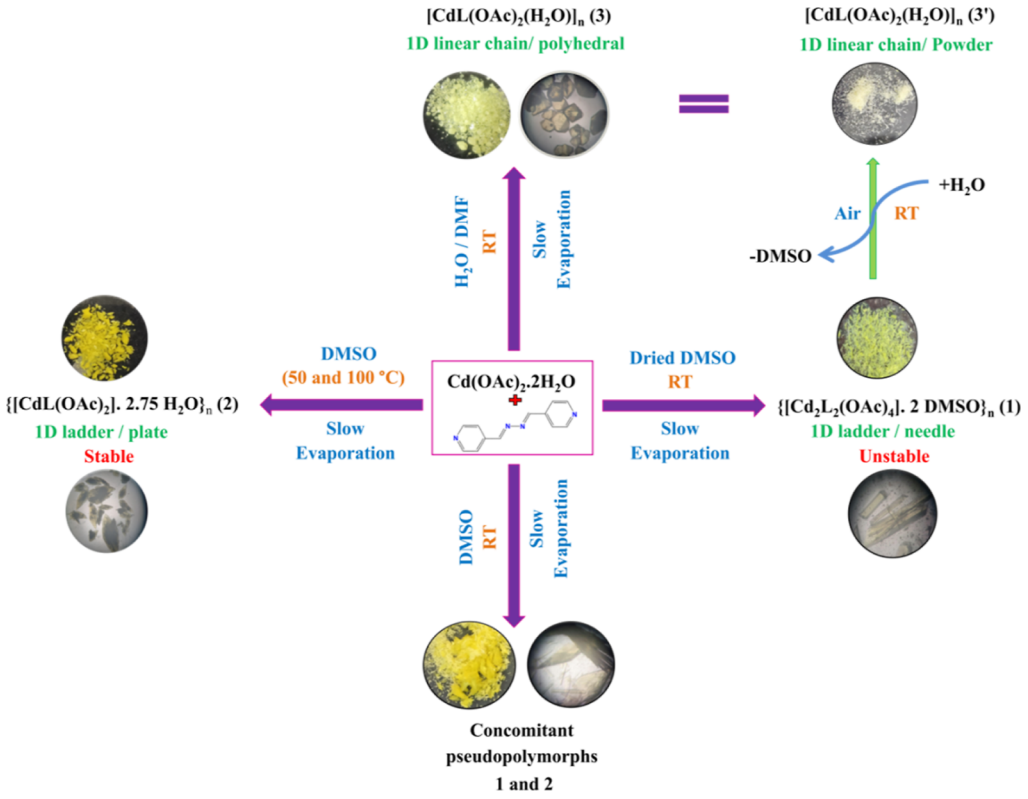

several months in air. Yields of 20 and 46% for compounds **1** and **2**, respectively, were obtained. mp: 252−256 and 258−259.5 °C for **1** and **2**, respectively. Elemental analysis for **2**: calculated: C, 39.20; H, 4.42; N, 11.43; found: C, 40.37; H, 3.38; N, 11.64. Elemental analysis for **1** was similar to **3′**.[28] FTIR (KBr, cm^{-1}) for compound **1**: 1602(s), 1567(s), 1416(s), 1345(w), 1310(m), 1229(m), 1056(w), 1009(m), 942(w), 880(w), 826(m), 679(s), 620(w), 543(m), 456(w) (Figure S1, Supporting Information). FTIR (KBr, cm^{-1}) for compound **2**: 3423(m), 1607(s), 1563(s), 1420(s), 1343(w), 1305(m), 1228(m), 1062(m), 1012(m), 950(m), 824(s), 737(w), 671(s), 618(m), 520(s), 460(m) (Figure S2, Supporting Information).

2.3. Synthesis of Pure $\{[Cd_2L_2(OAc)_4]\cdot 2DMSO\}_n$ (1). 0.0380 g (0.1426 mmol) of $Cd(OAc)_2.2H_2O$ and 0.030 g (0.1427 mmol) of **L** were dissolved in 1.5 mL of dried DMSO separately. It should be mentioned that the DMSO solvent was dehydrated by using an activated molecular sieve for several days. Then, the solution of ligand was added dropwise to the vial containing the solution of cadmium acetate. The resulted solution was stirred in room temperature for 30 min. After that, the solution was transferred to a clean vial containing 0.1 g of activated molecular sieve for capturing any probable water molecules from the salt and the environment. Then, the rim of the vial was sealed to avoid water absorption from air, and only three small holes were created on the rim. After 3 days, yellow needle-shaped crystals of compound **1** appeared purely without formation of compound **2** (yield 40%).

2.4. Synthesis of Pure $\{[CdL(OAc)_2]\cdot 2.75\ H_2O\}_n$ (2). Compound **2** was synthesized purely at a higher temperature (50 or 100 °C) by mixing 1:1 molar ratio of metal and ligand in DMSO according to the preparation method of concomitants **1** and **2** (yield 60%). Other experimental methods and reaction conditions that resulted in pure compound **2** are summarized in Table S1, Supporting Information.

2.5. Synthesis of $[CdL(OAc)_2(H_2O)]_n$ (3). Compound **3** was previously synthesized by Fonari[62] and us.[28] For the synthesis methods and characterization, please see our previous report[28] and Supporting Information.

2.6. Synthesis of Powder $[CdL(OAc)_2(H_2O)]_n$ (3′) from $\{[Cd_2L_2(OAc)_4]\cdot 2DMSO\}_n$ (1). As mentioned in the experimental section, single crystals of compound **1** were unstable after extracting from the mother solvent. After careful examination of the analysis results, it was found that compound **1** loses its free solvents after leaving the mother solvent and absorbs water molecules from the environment. Our results showed that single crystals of compound **1** completely transform to pure polycrystalline sample of compound **3** (**3′**).

3. SINGLE-CRYSTAL X-RAY DIFFRACTION STUDIES

Details of the single-crystal structure analysis for CPs **1**−**3** are given in the Supporting Information. Crystal data and refinement details for **1**−**3** are represented in Table 1. Selected bond lengths and angles for **1**−**3** are represented in Tables S2−S5, respectively. In order to clarify the structure of compound **3** and explain the transformation of compound **1** to **3**, we report a new data collection on compound **3**. Also, we report the crystal structure of **2** after removing free disordered solvent molecules by Squeeze using Platon[63] software as **2sq**.

4. RESULTS AND DISCUSSION

4.1. Synthesis of Compounds 1−3. Several 1D cadmium CPs containing 1,4-bis(4-pyridyl)-2,3-diaza-1,3-butadiene (**L**) have been reported previously.[16,28,62,64,65] Reaction of $Cd(OAc)_2\cdot 2H_2O$ and Schiff base ligand in DMSO (as purchased)

https://doi.org/10.1021/acsomega.3c00405
ACS Omega 2023, 8, 13140−13152

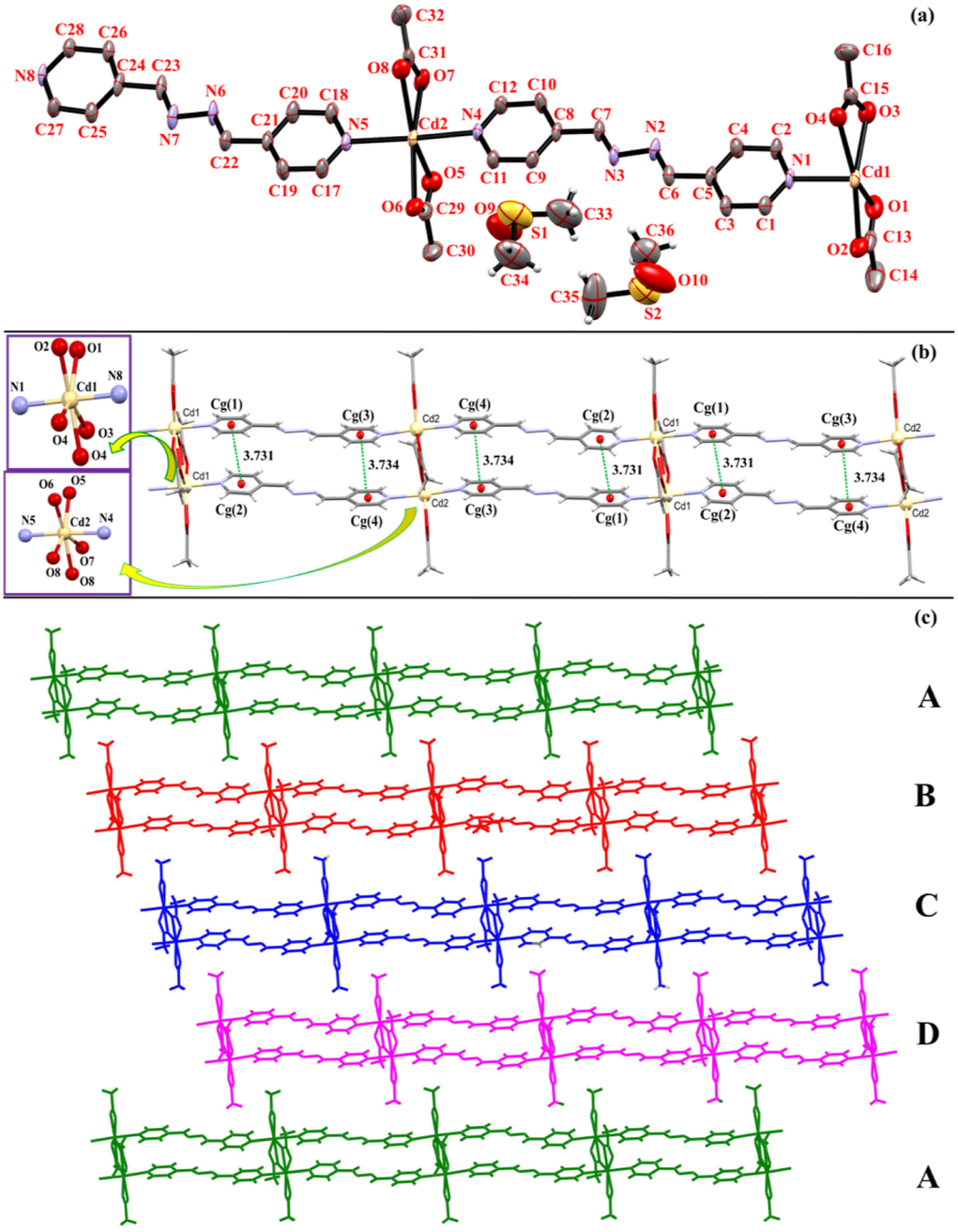

Figure 1. (a) ORTEP diagram of the asymmetric unit of **1**. Thermal ellipsoids are at 30% probability level. Hydrogen atoms of ligands and anions have been omitted for clarity. (b) 1D ladder of **1**, coordination environments of Cd(1) and Cd(2), and $\pi-\pi$ interactions between two pyridine rings of two parallel ligands. Cg(1): centroid of N(1)−C(1)−C(2)−C(3)−C(4)−C(5); Cg(2): centroid of N(8)−C(24)−C(25)−C(26)−C(27)−C(28); Cg(3): centroid of N(4)−C(8)−C(9)−C(10)−C(11)−C(12); Cg(4): centroid of N(5)−C(17)−C(18)−C(19)−C(20)−C(21). (c) Packing arrangement of 1D ladders in the ABCD form in **1**. DMSO solvent molecules have been omitted for clarity in (b, c).

at room temperature using the slow evaporation method resulted in concomitant formation of single crystals of **1** and **2**. Also, using a higher temperature (50 or 100 °C) without changing other factors resulted in **2** purely. In order to obtain crystals of **1** purely, dehydrated DMSO was used, and activated molecular sieve was added to the reaction vessel. Also, crystals of compound **1** completely transformed to a powder sample of **3** (**3′**) after extracting from the mother solvent and exposing them to air at ambient temperature. In contrast, crystals of compound **2** were stable at ambient temperature for several months (Scheme 1). Compound **3** (crystalline) and **3′** (powder) have been reported recently by our research group[28] and Fonari et al.[62]

4.2. Crystal Structure Analysis of Compounds 1−3. *4.2.1. Compound {[$Cd_2L_2(OAc)_4$]·2DMSO}$_n$ (1).* X-ray crystallography for the needle-shaped single crystals of compound **1** shows that it crystallizes in the triclinic crystal system and $P\bar{1}$ space group. The asymmetric unit contains two cadmium atoms, two **L**, four coordinated acetate anions, and two uncoordinated DMSO molecules (Figure 1a). There are two kinds of Cd(II) ions as metal centers; however, both have the same N_2O_5 coordination environment. They show coordination number 7, completed by two nitrogen atoms from

https://doi.org/10.1021/acsomega.3c00405
ACS Omega 2023, 8, 13140−13152

Table 2. Hydrogen Bond Parameters (Y−A···H−D) for Compound 1[a]

D−H···A	d (D−H)/Å	d (H···A)/Å	d (D···A)/Å	<(DHA)/°
C(9)−H(9)···O(9)	0.93	2.62	3.288(18)	129
C(22)−H(22)$^{\#1}$···O(9)	0.93	2.63	3.26(2)	126
C(6)−H(6)···O(10)	0.93	2.85	3.486(2)	126
C(25)−H(25)$^{\#1}$···O(10)	0.93	2.73	3.412(2)	131
C(35)−H(35B)$^{\#2}$···O(1)	0.96	2.71	3.639(2)	162
C(10)−H(10)···O(1)$^{\#3}$	0.93	2.53	3.414(14)	159

[a]Symmetry codes: #1: 2 − *x*, 2 − *y* + 1, 1 − *z*; #2: 1 − *x*, 1 − *y*, 2 − *z*; #3: −*x*, −*y* + 1, −*z* + 2.

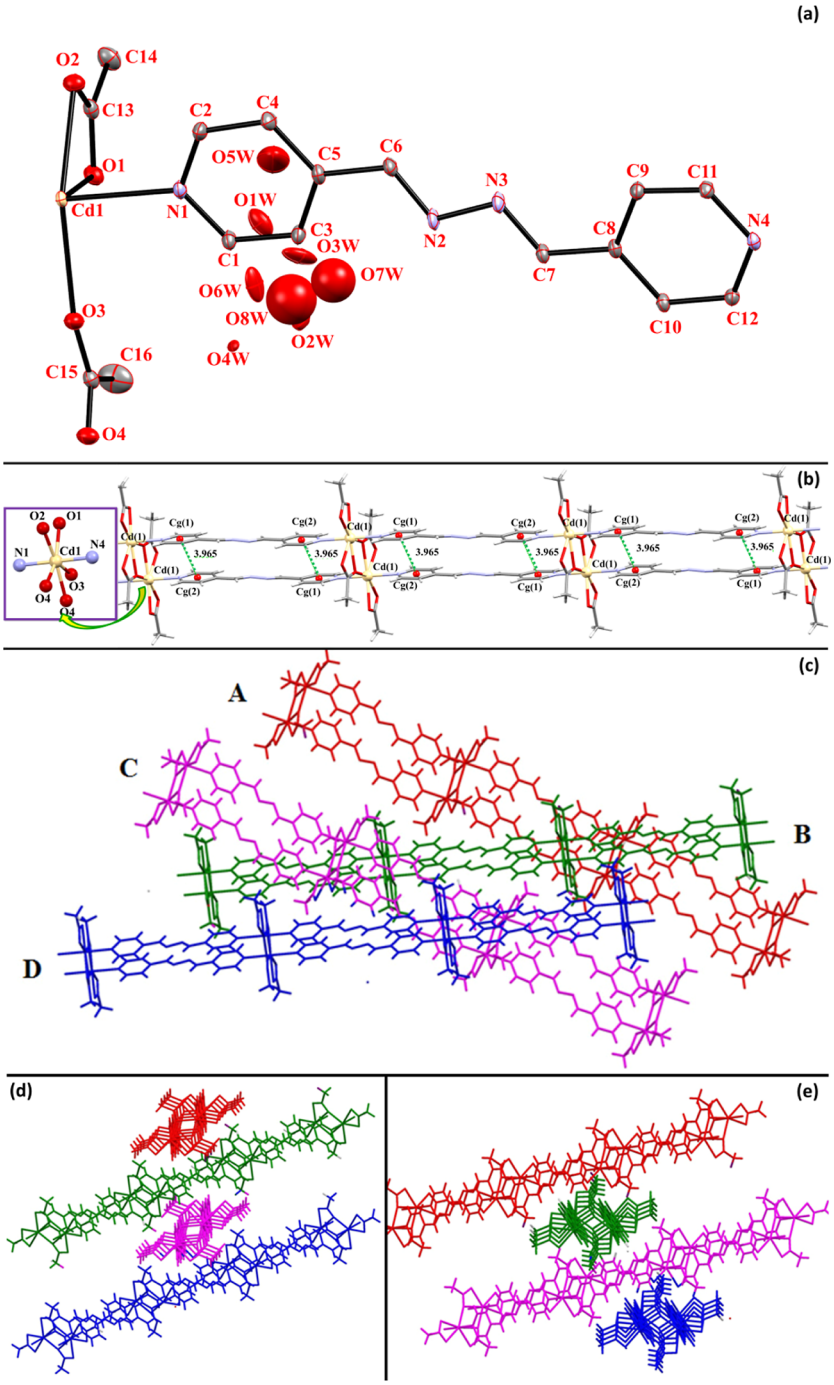

Figure 2. (a) ORTEP diagram of the asymmetric unit of **2**. Thermal ellipsoids are at 30% probability level. Hydrogen atoms have been omitted for clarity. (b) 1D ladder of **2** and coordination environment of the metal center. Cg−Cg distance between two pyridine rings of two **L** in the ladder structure. Cg(1): centroid of N(1)−C(1)−C(2)−C(3)-C(4)−C(5); Cg(2): centroid of N(4)−C(8)−C(9)−C(10)−C(11)−C(12). (c−e) Packing arrangements of 1D ladders in the ABCD form in **2** from different views.

https://doi.org/10.1021/acsomega.3c00405
ACS Omega 2023, 8, 13140−13152

pyridine rings of two **L** and five oxygen atoms of three acetate anions that form a distorted pentagonal-bipyramidal geometry (Figure 1b). Important bond angles and bond distances for compound **1** are listed in Table S2, Supporting Information. As shown in Figure 1b, the structure of compound **1** is extended only by ligand **L** in one dimension. Two acetate anions are bridged between cadmium centers via the coordination mode of the chelate bridge, and two others exhibit the chelate coordination mode. Although acetate anions do not participate in the extension of structure, their presence and unique coordination pattern resulted in the 1D ladder CP (Figure 1b).[16,28,66] As shown in Figure 1a, DMSO solvent molecules are present in the structure as guests. Their locations between ladder motifs are shown in Figure S4, Supporting Information. In the crystal structure of compound **1**, $\pi-\pi$ interactions are also found between two pyridine rings of two parallel ligands in the ladder structure. These $\pi-\pi$ interactions can be classified as head-to-head ones.[67] The pyridine rings involved in aromatic−aromatic interactions are almost face-to-face[67] with the Cg(1)−Cg(2) distance of 3.731(6) Å and the Cg(3)−Cg(4) distance of 3.734(6) Å (Figure 1b). Investigation of the packing of **1** shows that the arrangement of ladders is in a parallel ABCD form (Figure 1c). The simplified image of the structural motif and the packing arrangement in compound **1** drawn by Topos software[68] are shown in Figure S5, Supporting Information.

Also, a close investigation of the structure of compound **1** reveals some weak C−H···O hydrogen bonds between the DMSO guest molecules and the ladder framework (Table 2 and Figure S6). It seems that these weak hydrogen bonds cannot sufficiently stabilize the crystal lattice in compound **1**. Since these interactions are weak, they easily allow the guest solvent to leave the network, and this phenomenon causes the destruction of the structure and its transformation into another structure. This structural transformation will be discussed in the following sections.

4.2.2. Compound $\{[CdL(OAc)_2]\cdot 2.75H_2O\}_n$ *(**2**).* X-ray crystallography for **2** reveals that it crystallizes in the monoclinic crystal system and $I2/a$ space group. The asymmetric unit contains one cadmium atom, one **L**, two coordinated acetate anions, and several uncoordinated water molecules (Figure 2a). Since free water molecules were disordered, they were removed by Squeeze program of Platon software[63] (compound **2sq**). Coordination environment around the metal center was a distorted (N_2O_5) pentagonal bipyramid, and the metal center is 7-coordinated as described for **1** (Figure 2b).

Some important bond distances and angles for **2** and **2sq** are listed in Tables S3 and S4, Supporting Information. In this compound, ligand **L** extended the polymeric structure in one dimension by two pyridine rings which formed a bridge between the two metal centers. The acetate anions bridge the two metal centers similar to compound **1** (Figure 2b). In **2**, the aromatic−aromatic distance (Cg(1)−Cg(2) = 3.965 Å) is outside the range acceptable for the interaction to take place.[67] Also, unlike compound **1**, parallel pyridine rings are displaced (Figure 2b).

X-ray crystallographic analysis of compounds **1** and **2** revealed that these concomitant compounds are pseudopolymorphs as they have the same structural motif with different guest molecules (DMSO for **1** and H_2O for **2**). Packing investigation of compound **2** shows that the ladder arrangement is totally different from compound **1** and can be described as an inclined ABCD form. As shown in Figure 2c−e, ladders A and B make an angle of about 50° with respect to each other, and ladders A and C are in the same direction, but the locations of the metal centers in these ladders are different in a way that the metal center in C is located in the middle of A. Ladders A and D not only make an angle of about 50° with respect to each other, but also the locations of the metal centers in these ladders are different. It should be noted that the same pattern is repeated among other layers in the structure of **2**. Simplified images of structural motifs and packing arrangement for compound **2** are shown in the Supporting Information (Figure S7). The search for the reasons for forming this unusual packing of **2**, which is completely different from **1**, led us to investigate different interactions in this structure. Probably, C−H···O hydrogen bonding between adjacent ladder motifs in compound **2** is the main reason for inclined ABCD packing (Table 3 and Figure 3). As a result, in **2**, hourglass-like channels were formed, filled by disordered water guest molecules (Figures 4 and 5). Using **2sq** cif file (after Squeeze of guests) and Mercury software,[69] it was determined that 15.7% of the unit cell volume (631.93 $Å^3$) is empty. This volume is equivalent to the space created by the inclined packing of ladders and occupied by the disordered guest water molecules (Figure 5).

Table 3. Hydrogen Bond Parameters (Y−A···H−D) for Compound 2[a]

D-H···A	d (D−H)/Å	d (H···A)/Å	d (D···A)/Å	<(DHA)°
C(4)−H(4)···O(1)	0.95	2.50	3.387(3)	156
C(10)−H(10)···O(4)$^{\#1}$	0.95	2.48	2.999(3)	115
C(10)−H(10)···O(2)$^{\#2}$	0.95	2.51	3.269(3)	137
C(7)−H(7)···O(4)	0.95	2.71	3.154	109

[a]Symmetry codes: #1: 3/2 − *x*, *y*, 1 − *z*, #2: *x*, 1/2 − *y*, 1/2 + *z*.

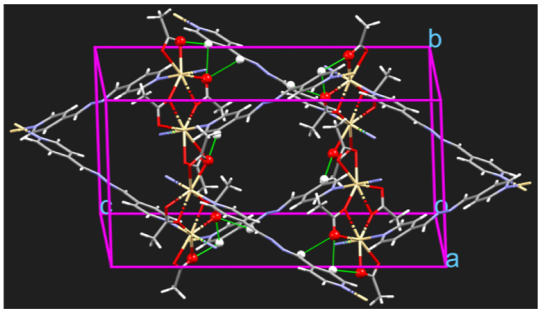

Figure 3. C−H···O hydrogen bonding between adjacent ladder motifs in compound **2**. Hydrogen bonds are shown as green dashed lines.

4.2.3. Compound $[CdL(OAc)_2(H_2O)]_n$ *(**3**) and **3**′.* In order to clarify the structure of compound **3** and to stress its importance in transformation studies, we report a new data collection. As we reported previously,[28] crystal structural analysis shows that the compound is C_2-symmetrical, and the coordination environment of cadmium atoms contains two ligand, two acetate anions, and one coordinated water molecule (Figure 6a). In contrast to compounds **1** and **2**, in the case of **3**, a distorted pentagonal-bipyramidal geometry (7 coordination number) was formed by four oxygen atoms of

https://doi.org/10.1021/acsomega.3c00405
ACS Omega 2023, 8, 13140−13152

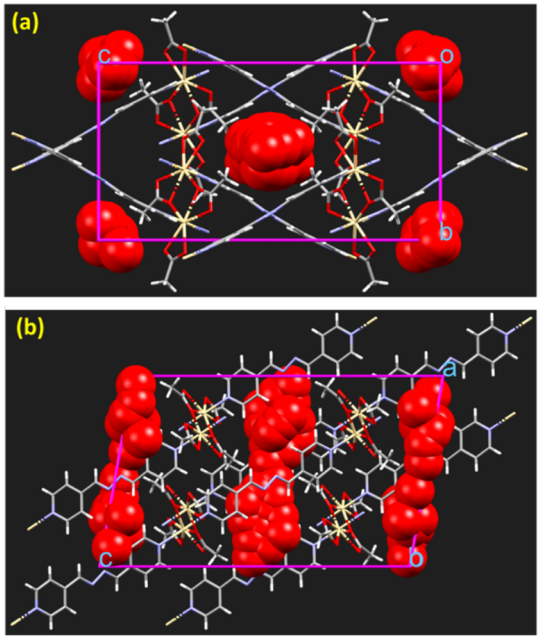

Figure 4. View of the disordered guest water molecules located in the 1D channel of **2**. (a) View along the crystallographic *a*-axis. (b) View along the crystallographic *b*-axis. For more clarity, water molecules are illustrated in the space filling mode.

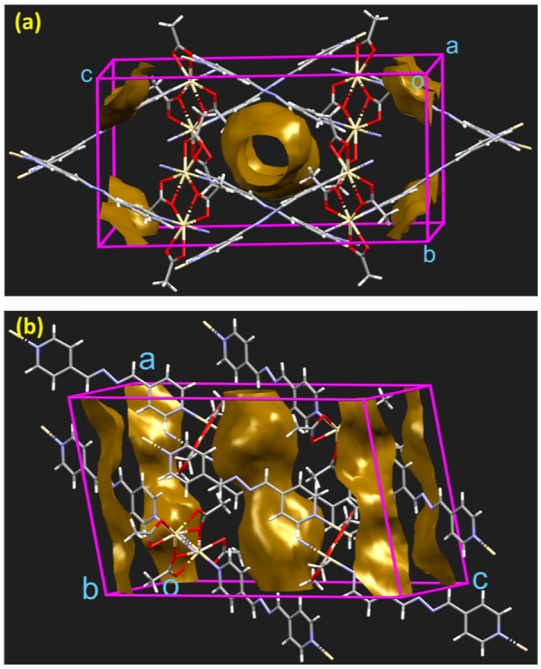

Figure 5. (a) View of channels along the crystallographic *a*-axis in **2sq**. Contact surfaces are illustrated by gold color. (b) View of the hourglass-like channels along the *c*-axis in **2sq**.

two acetate anions, two pyridine rings of two ligand **L**, and one oxygen atom from the coordinated water molecule (Figure 6b). Information related to bond distances and angles for **3** are listed in Table S5, Supporting Information. Figure 6b shows that compound **3** expands through the ligand in one dimension and forms a 1D polymeric linear chain. Further investigation about the crystal structure description and important interactions of **3** has been reported in our previous work.[28] It should be noted that the crystal structure of **3′** (polycrystalline form of **3**) has been determined by the Rietveld method previously.[28]

4.3. Controlling Role of Water Content and Temperature in the Formation of Concomitant vs Pure Form of Pseudopolymorphs 1 and 2. Since water was not used as the solvent in the experimental process, it seems that water guest molecules in the lattice of **2** were absorbed from humidity in air, DMSO solvent, or cadmium acetate hydrate salt. The interesting point is that the presence of water molecules in the self-assembly process creates a concomitant formation of pseudopolymorphs which—to the best of our knowledge—is quite unique. For more investigation and to understand the role of humidity, water molecules were removed from DMSO and cadmium acetate salt by using an activated molecular sieve and sealing the rim of the sample to avoid absorbing water from air. As a result of removing water from the reaction vessel, only crystals of compound **1** have been formed and crystals of **2** could not be obtained. As mentioned, compound **2** was formed almost 4 days after compound **1**. Since the time of formation and the applied temperature used in the reaction are two main factors in understanding the stability of compounds[70] and, for most of the time, more stable compounds have been prepared at higher temperature,[70−74] it made us consider that probably **2** is more stable than **1**. For more investigation, the test was repeated for the synthesis of **1** and **2** in DMSO at 50 and 100 °C which led to interesting findings. In these higher temperatures, only compound **2** was obtained. This result shows that formation of compound **2** needs either more time (1 week) at low temperature (RT) or higher temperature in comparison with compound **1**. In all reactions, the presence of a small amount of moisture (as impurity) in the reaction container was found to be necessary for the formation of compound **2** in pure or concomitant form.

4.4. Investigation of the Morphology and Stability of Concomitant Pseudopolymorphs 1 and 2. As mentioned, both compounds **1** and **2** have shown 1D ladder structural motif with different guest solvent molecules (DMSO for **1** and H_2O for **2**) which confirms that they are pseudopolymorph supramolecular isomers. Our results show that in our case, differences in guest solvents did not affect the structural motif significantly but affect the pattern of arrangement of 1D ladders. Also, guest solvents affected the morphology and stability of compounds **1** and **2**. The optical microscope images have shown that compounds **1** and **2** have needle and plate shapes, respectively (Figure 7a). For further investigation, SEM image of the sample containing two compounds **1** and **2** was taken, which clearly shows the difference in morphology (Figure 7b). Although the fact that the solvent used in the reaction affects the morphology of CPs was previously confirmed by our team,[16,23] this work showed that even guest solvents can affect the morphology of pseudopolymorph CPs.

Another interesting point is about the role of guest water solvents in the stability of compound **2**. Interestingly, when single crystals of **2** were separated from the mother solvent, they kept their crystal shape and brilliance at an ambient temperature for several months. In contrast, single crystals of **1** lost their transparency gradually after extraction from the solvent. These evidences show that compound **2** is more stable than compound **1** in air. This fact led us to the conclusion that despite the higher boiling point of DMSO, probably free water molecules increase the stability of compound **2** through strong

https://doi.org/10.1021/acsomega.3c00405
ACS Omega 2023, 8, 13140−13152

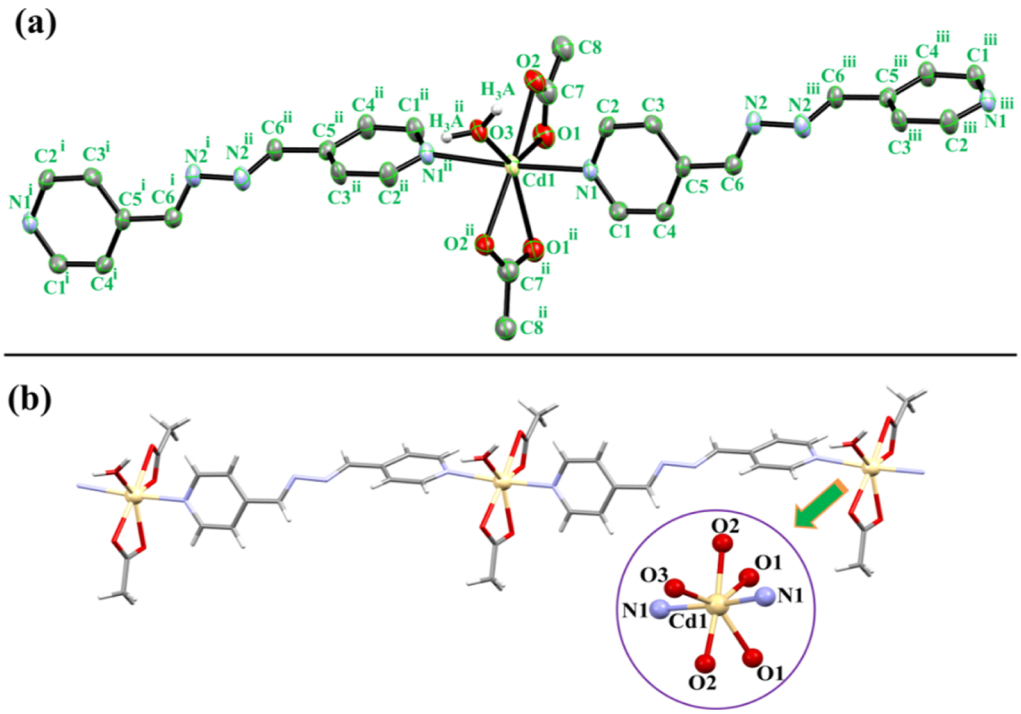

Figure 6. (a) ORTEP of the coordination environment of cadmium atom in **3**. Symmetry codes: (i): 1 + *x*, 1 + *y*, *z*, (ii): 2.5 − *x*, 2 − *y*, *z*, (iii): 1.5 − *x*, 1 − *y*, *z*. (b) Linear chain and N_2O_5 geometry of cadmium centers in **3**.

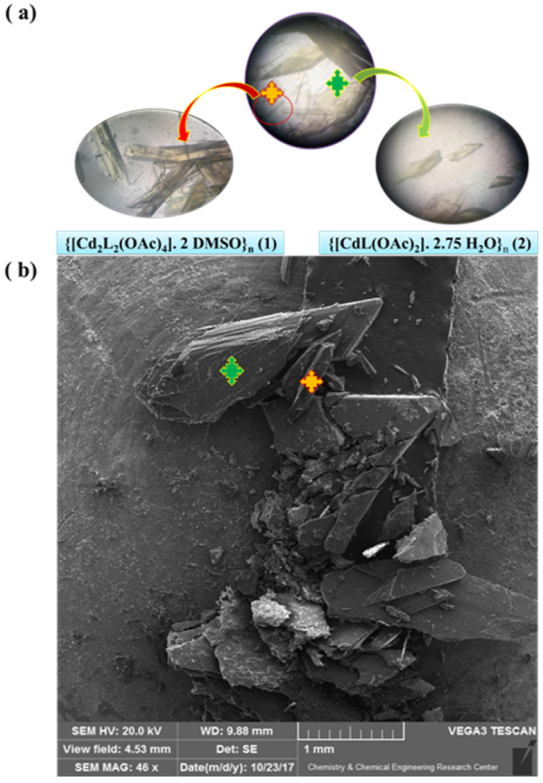

Figure 7. Images of (a) the optical microscope and (b) SEM of sample containing pseudopolymorphs of **1** and **2**.

hydrogen bonds between themselves and also with the electronegative atoms of the structural framework. Unfortunately, the free water molecules were disordered in structure, and it was not possible to describe the details of their hydrogen bonds in this paper.

4.5. Structural Transformation Studies. *4.5.1. Single Crystal-to-Powder Transformation (**1** to **3**′).* As mentioned in previous sections, compound **1** was unstable after extracting from the mother solvent and exposing to air. After the preliminary examination of the powder diffractograms of compound **1** before and after grinding, a significant mismatch with the simulated pattern of compound **1** was observed. Since we had recently observed a similar phenomenon in the compounds of this family,[28] by comparing the results of FTIR, TGA, and XRD analyses of the powder sample of compound **1** with compound **3** (single crystal of **3**′), we realized that they are the same. It means that when unstable crystals of compound **1** are extracted from the mother solvent and exposed to air, they lose their lattice solvent (in this case DMSO), absorb water molecules from air, and transform to **3**′ (powder form of **3**). Because the sample loses its single-crystal state during the transformation, this is considered as single crystal-to-powder transformation. In the previous article, we have determined the structure of a powder sample similar to sample **3**′ by the Rietveld method.[28]

4.5.1.1. PXRD Studies. The XRD analysis for compound **1** was performed when it was extracted from the reaction vessel (at the beginning of transformation). As shown in Figure 8, there was some agreement between experimental and simulated XRD patterns. The differences and unknown peaks could be attributed to the beginning of the transformation. The XRD analysis was carried out again when the crystals of **1** were exposed to air and lost their crystal shape and lattice solvents. XRD analyses showed that it was completely different from the simulated XRD pattern of **1** and was similar to the XRD pattern of compound **3**. Since all characterizations of the new powder of compound **1** (**3**′) were in agreement with the crystals of **3**, and also in the previous work, the structure determination of the same powder sample was done by Rietveld method,[28] it was not deemed necessary to do it again.

https://doi.org/10.1021/acsomega.3c00405
ACS Omega 2023, 8, 13140−13152

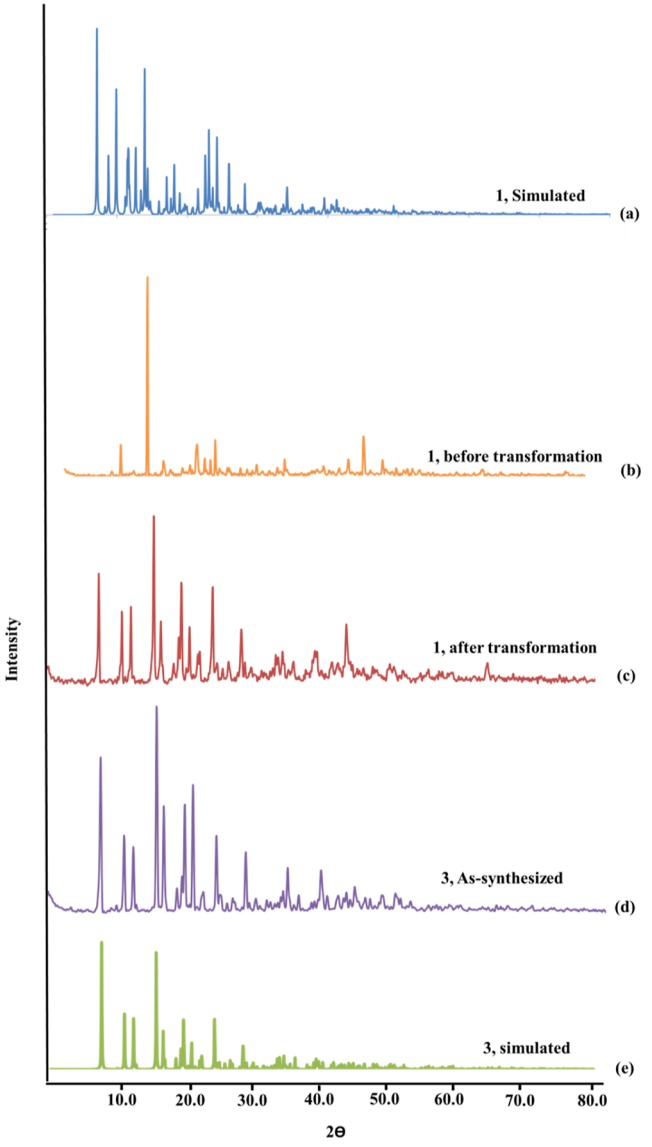

Figure 8. Experimental XRD patterns of crystals of compound **1** (b) immediately after synthesis and without grinding and (c) after exposure to air and grinding. (a, e) Simulated XRD patterns of **1** and **3**. (d) Experimental XRD pattern of crystal **3**.[28]

The simulated XRD analysis for the as-synthesized compound and compound **2** were in good agreement and confirmed that compound **2** was pure and stable even after grinding (Figure 9).

4.5.1.2. TGA. Since compound **1** was unstable after leaving the mother solvent and quickly transformed into compound **3′**, it was not possible to perform TGA for the sample before transformation. So, TGAs for compound **1** (after transformation) and for compound **2** were performed in the range of 25−700 °C under N_2 and 10 °C/min heating rate (Figure 10). Also, TGA analysis for compound **3′** was performed previously[28] at the same range, and the results showed a similar thermal behavior of **1** (after transformation) and **3′** (Figure 10). Figure 10 shows that the TGA curves of compounds **3′** and **1** (after transformation) are similar. These results testify for the transformation from **1** to **3′**. The thermal behavior curve for compound **2** shows that this compound is stable until 190 °C and the water molecule does not leave the structure until this temperature. This result confirms that

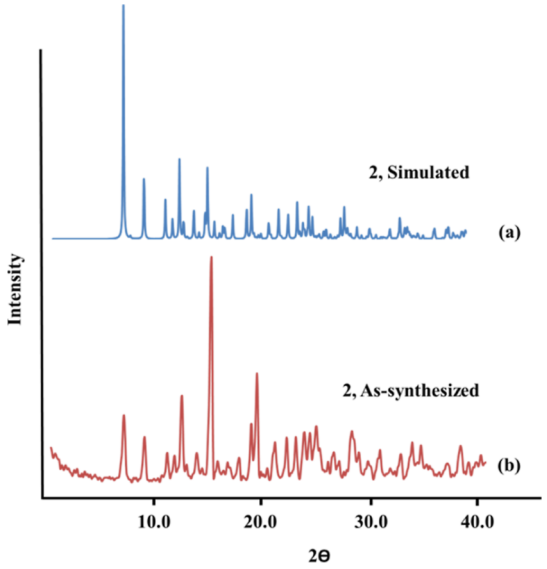

Figure 9. XRD patterns of compound **2**. (a) Simulated pattern. (b) Experimental pattern.

probably there are strong hydrogen bonds in the lattice that made the guest water molecules nonvolatile until around 190 °C and made the structure stable. Also, TGA confirms that there are almost three water molecules in the structure. The first weight loss step of 34.78 wt % occurred in the range of 190−280 °C and is associated with the release of three water molecules and two acetate anions in two steps (calc. 34.97 wt %).

4.5.1.3. FTIR Analysis. FTIR analyses were performed for better understanding of the synthesized compounds and transformation process by using assignments reported in the literature.[75,76] FTIR spectra of compounds **1** and **2** exhibit signals related to the ligands and acetate anions (Figures S1 and S2). The band around 1600−1610 cm^{-1} corresponds to the stretching mode of Schiff base bond (C═N) in the ligand. Also, the bands around 1565−1570 and 1415−1420 cm^{-1} can be related to the stretching modes of the acetate anions. As expected, the FTIR spectra of compound **1** do not show any bands corresponding to free DMSO molecules.[75,76] Instead, a broad band related to coordinated water molecules appears at around 3200 cm^{-1}(ca. 3300−3000)[76] in compound **1** after exposing to air and grinding (Figures 11 and S1, Supporting Information). In addition, comparison of the FTIR spectra of compounds **1** and **3′** revealed that they are similar (Figure 11). Hence, FTIR spectra are another witness for the transformation of **1** to **3** (**3′**). In compound **2** (Figure S2), a broad band related to uncoordinated water molecules appears at around 3400 cm^{-1}(ca. 3550−3200).[76]

4.5.2. DRST. In order to investigate the transformation of compound **3** to **1** and **2** through the DRST process, several single crystals of **3** were immersed and dissolved in DMSO and DMF at 100 °C. After 1 week, new yellow plate-shaped crystals were obtained in both the solutions (Figure 12). Single-crystal X-ray analysis of these crystals showed that they are the same as compound **2**. This result clarified that transformation from **3** to **2** is possible through the DRST process. The result of synthetic experiments and structural transformations using the DRST method showed that the amount of water in the reaction container plays an important role in the formation of one of the compounds **2** (uncoordinated water) or **3**

https://doi.org/10.1021/acsomega.3c00405
ACS Omega 2023, 8, 13140−13152

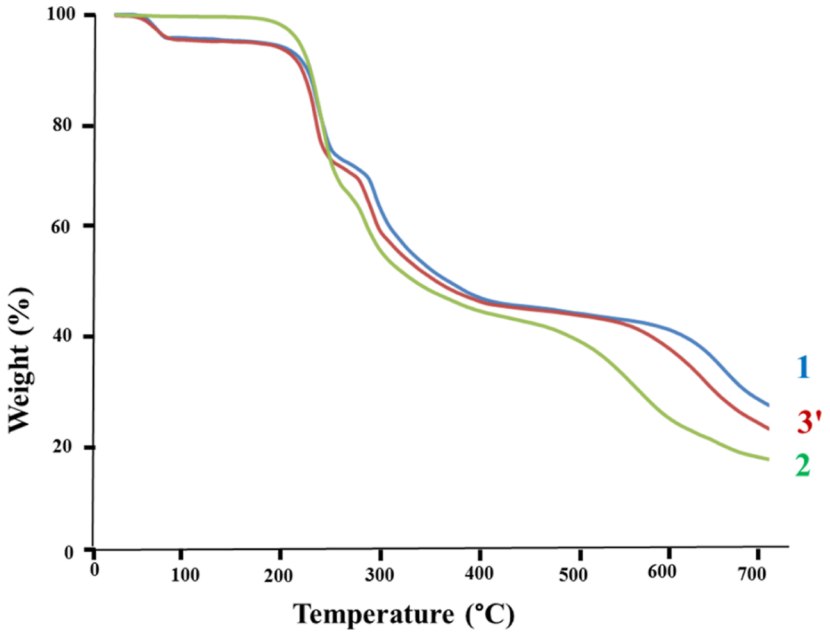

Figure 10. Comparison of TGA for compounds **1**, **2**, and **3′**.[28]

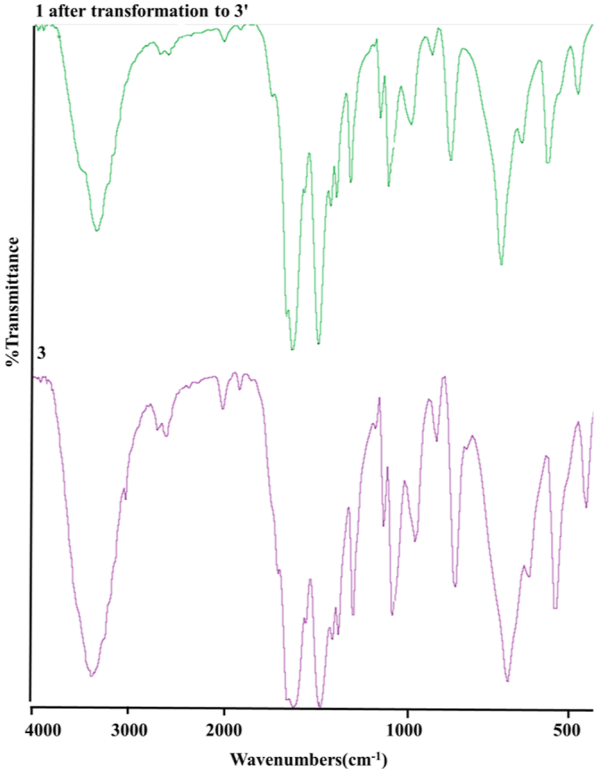

Figure 11. FTIR analyses of **1** after transformation to **3′** and **3**.[28]

(coordinated water). If a significant amount of water (reaction solvent) is present, compound **3** will be synthesized as a pure compound. Whereas if a small amount of water is present in the system through absorption from air or solvent impurity, compound **2** is specifically prepared as the exclusive product.

A proof of this claim is the transformation of compound **3** to compound **2** through DRST in DMF or DMSO, in which the reaction environment has a low amount of water. Also, in all synthesis methods to obtain compound **2**, which is given in

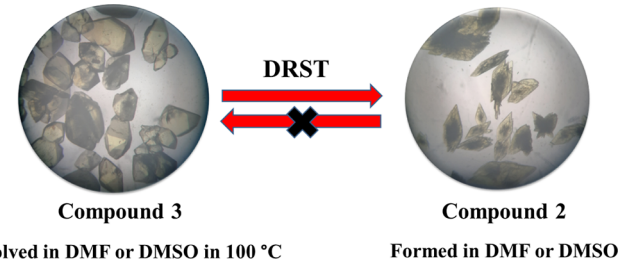

Figure 12. DRST process for transforming compound **3** to compound **2**.

Table S1 (Supporting Information), only minor amounts of water are present (Scheme 2).

Scheme 2. Transformation Routes of 3 to 2 through the DRST Process and the Role of Amount of Water in Creating 2 versus 3

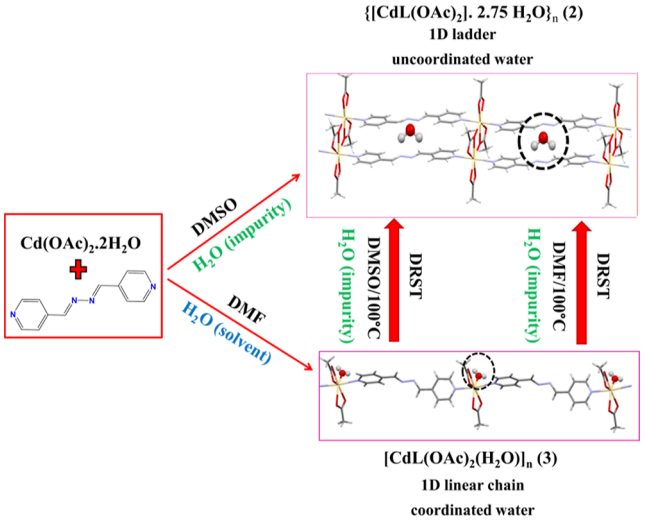

https://doi.org/10.1021/acsomega.3c00405
ACS Omega 2023, 8, 13140−13152

5. CONCLUSIONS

In summary, we reported the synthesis of two concomitant pseudopolymorph CPs $\{[Cd_2L_2(OAc)_4]\cdot 2DMSO\}_n$ (**1**) and $\{[CdL(OAc)_2]\cdot 2.75H_2O\}_n$ (**2**) through the self-assembly process in the DMSO solvent. Structure analysis for compounds **1** and **2** revealed the formation of 1D ladder motif for the pseudopolymorphs **1** and **2** containing DMSO and water guest solvents, respectively. Our study showed that the presence of water impurity in DMSO plays an important role in the formation of compound **2** and also creating the possibility of formation of concomitant pseudopolymorphs **1** and **2**. Our analyses revealed that compound **2** is more stable than compound **1**. In contrast to compound **2**, compound **1** was unstable in air at room temperature. Environmental humidity provided the driving force for the single crystal-to-powder transformation of **1** (1D ladder) to **3′** (1D linear chain) after extracting **1** from the mother solvent and exposing to air. Also, we showed that compound **3** transformed to compound **2** in DMF or DMSO through the DRST process. The result of synthetic experiments and structural transformations using the DRST method showed that the water content in the reaction container plays an important and decisive role in the formation of one of the compounds **2** (uncoordinated water) or **3** (coordinated water). If a significant amount of water (as reaction solvent) is present, compound **3** will be synthesized as a pure compound. Whereas if a small amount of water is present (through absorption from air or solvent impurity), compound **2** is specifically prepared as the exclusive product.

ASSOCIATED CONTENT

Supporting Information

The Supporting Information is available free of charge at https://pubs.acs.org/doi/10.1021/acsomega.3c00405.

Location of the guest solvents in the packing of compound **1**, other techniques and synthesis methods for compounds **2** and **3**, simplified packing arrangement in compounds **1** and **2**, selected bond lengths and angles, and also additional details of X-ray crystallography and FTIR for all compounds (PDF)

Crystallographic information for **1** (CIF)

Crystallographic information for **2** (CIF)

Crystallographic information for **2sq** (CIF)

Crystallographic information for **3** (CIF)

AUTHOR INFORMATION

Corresponding Author

Behrouz Notash − *Department of Inorganic Chemistry, Shahid Beheshti University, 1983969411 Tehran, Iran;* orcid.org/0000-0003-4873-5770; Phone: +98 2129904363; Email: b_notash@sbu.ac.ir; Fax: +98 2122431663

Authors

Mona Farhadi Rodbari − *Department of Inorganic Chemistry, Shahid Beheshti University, 1983969411 Tehran, Iran*

Maciej Kubicki − *Faculty of Chemistry, Adam Mickiewicz University, 61-614 Poznań, Poland*

Complete contact information is available at: https://pubs.acs.org/10.1021/acsomega.3c00405

Notes

The authors declare no competing financial interest.

ACKNOWLEDGMENTS

We thank the Graduate Study Councils of Shahid Beheshti University for financial support.

REFERENCES

(1) Batten, S. R.; Neville, S. M.; Turner, a. D. R. *Coordination Polymers Design, Analysis and Application*; Royal Society of Chemistry: Cambridge, U.K. 2009.

(2) De La Pinta, N.; Klar, P. B.; Breczewski, T.; Madariaga, G. Host Polytypism and Structural Modulation in Two-Dimensional Fe(NCS)2-Based Metal-Organic Frameworks: Can Spin-Crossover Transitions Be Predicted? *Cryst. Growth Des.* **2020**, *20*, 422−433.

(3) Cheng, J.-G.; Liu, J.; Tong, W.-Q.; Wu, D.; Yang, F.; Hou, L.; Wang, Y.-Y. Two new MOFs based on 5-((4-carboxypyridin-2-yl)oxy) isophthalic acid displaying unique selective CO_2 gas adsorption and magnetic properties. *CrystEngComm* **2019**, *21*, 7078−7084.

(4) Chakraborty, T.; Sarkar, A.; Adhikary, A.; Chakiroy, N.; Das, D. Synthesis of Structurally Diverse Ferrimagnetically and Antiferromagnetically Coupled M^{II}-Mn^{II} (M = Cu, Ni) Heterometallic Schiff Base Compounds with a Dicyanamide Spacer and Study of Biomimetic Catalytic Activity. *Cryst. Growth Des.* **2019**, *19*, 7336−7348.

(5) Derakhshandeh, P. G.; Abednatanzi, S.; Leus, K.; Janczak, J.; Van Deun, R.; Van Der Voort, P.; Van Hecke, K. Ce(III)-Based Frameworks: From 1D Chain to 3D Porous Metal-Organic Framework. *Cryst. Growth Des.* **2019**, *19*, 7096−7105.

(6) Alavijeh, R. K.; Akhbari, K.; White, J. Solid-Liquid Conversion and Carbon Dioxide Storage in a Calcium-Based Metal-Organic Framework with Micro- and Nanoporous Channels. *Cryst. Growth Des.* **2019**, *19*, 7290−7297.

(7) Baig, F.; Rangan, K.; Eappen, S. M.; Mandal, S. K.; Sarkar, M. Template effect of innocent and coordinating anions on the formation of interpenetrated 2D and 3D networks: methyl orange and iodine sorption studies. *CrystEngComm* **2020**, *22*, 751−766.

(8) Wang, S.; Liu, J.; Zhao, H.; Guo, Z.; Xing, H.; Gao, Y. Electrically Conductive Coordination Polymer for Highly Selective Chemiresistive Sensing of Volatile Amines. *Inorg. Chem.* **2018**, *57*, 541−544.

(9) Halder, S.; Dey, A.; Bhattacharjee, A.; Ortega-Castro, J.; Frontera, A.; Ray, P. P.; Roy, P. A Cd(II)-based MOF as a photosensitive Schottky diode: experimental and theoretical studies. *Dalton Trans.* **2017**, *46*, 11239−11249.

(10) Dutta, B.; Hazra, A.; Dey, A.; Sinha, C.; Ray, P. P.; Banerjee, P.; Mir, M. H. Construction of a Succinate-Bridged Cd(II)-Based Two-Dimensional Coordination Polymer for Efficient Optoelectronic Device Fabrication and Explosive Sensing Application. *Cryst. Growth Des.* **2020**, *20*, 765−776.

(11) Gayathri, P.; Karthikeyan, S.; Pannipara, M.; Al-Sehemi, A. G.; Moon, D.; Anthony, S. P. Aggregation-enhanced emissive mechanofluorochromic carbazole-halogen positional isomers: tunable fluorescence via conformational polymorphism and crystallization-induced fluorescence switching. *CrystEngComm* **2019**, *21*, 6604−6612.

(12) Leong, W. L.; Vittal, J. J. One-Dimensional Coordination Polymers: Complexity and Diversity in Structures, Properties, and Applications. *Chem. Rev.* **2011**, *111*, 688−764.

(13) Zhao, J.; Yuan, J.; Fang, Z.; Huang, S.; Chen, Z.; Qiu, F.; Lu, C.; Zhu, J.; Zhuang, X. One-dimensional coordination polymers based on metal-nitrogen linkages. *Coord. Chem. Rev.* **2022**, *471*, 214735.

(14) Notash, B.; Safari, N.; Khavasi, H. R. Anion-controlled structural motif in one-dimensional coordination networks via cooperative weak noncovalent interactions. *CrystEngComm* **2012**, *14*, 6788−6796.

(15) Desai, A. V.; Sharma, S.; Roy, A.; Ghosh, S. K. Probing the Role of Anions in Influencing the Structure, Stability, and Properties in Neutral N-Donor Linker Based Metal-Organic Frameworks. *Cryst. Growth Des.* **2019**, *19*, 7046−7054.
(16) Notash, B.; Farhadi Rodbari, M. Anion-controlled structural motifs in cadmium coordination polymers: Formation of linear chain versus triple-stranded ladder. *Polyhedron* **2019**, *171*, 260−268.
(17) Li, G.-B.; Yang, Q.-Y.; Pan, R.-K.; Liu, S.-G. Diverse cobalt(II) coordination polymers for water/ethanol separation and luminescence for water sensing applications. *CrystEngComm* **2018**, *20*, 3891−3897.
(18) Li, Q.; Wu, X.; Huang, X.; Xiao, X.; Jia, S.; Lin, Z.; Zhao, Y. Temperature-Driven Crystal-to-Crystal Transformations and Luminescence Properties of Coordination Polymers Built with Diphenyldibenzofulvene Based Ligand. *Cryst. Growth Des.* **2018**, *18*, 912−920.
(19) Li, S.-L.; Han, M.; Wu, B.; Wang, J.; Zhang, X.-M. Photochromic Porous and Nonporous Viologen-Based Metal-Organic Frameworks for Visually Detecting Oxygen. *Cryst. Growth Des.* **2018**, *18*, 3883−3889.
(20) Liu, X.; Ma, X.; Yang, J.; Luo, S.; Wang, Z.; Ferrando-Soria, J.; Ma, Y.; Shi, Q.; Pardo, E. Solvent-induced single-crystal-to-single-crystal transformation and tunable magnetic properties of 1D azido-Cu(II) chains with a carboxylate bridge. *Dalton Trans.* **2019**, *48*, 11268−11277.
(21) Li, C.-P.; Ai, J.-Y.; He, H.; Li, M.-Z.; Du, M. Divergent Structural Transformations in 3D Ag(I) Porous Coordination Polymers Induced by Solvent and Anion Exchanges. *Cryst. Growth Des.* **2019**, *19*, 2235−2244.
(22) Lee, H. G.; Jo, H.; Eom, S.; Kang, D. W.; Kang, M.; Hilgar, J.; Rinehart, J. D.; Moon, D.; Hong, C. S. Cyclic Structural Transformations from Crystalline to Crystalline to Amorphous Phases and Magnetic Properties of a Mn(II)-Based Metal-Organic Framework. *Cryst. Growth Des.* **2018**, *18*, 3360−3365.
(23) Notash, B.; Rezaei Kheirkhah, B. The effect of solvent on one-dimensional cadmium coordination polymers. *New J. Chem.* **2018**, *42*, 15014−15021.
(24) Zhang, J.-P.; Huang, X.-C.; Chen, X.-M. Supramolecular isomerism in coordination polymers. *Chem. Soc. Rev.* **2009**, *38*, 2385−2396.
(25) Park, I.-H.; Ju, H.; Herng, T. S.; Kang, Y.; Lee, S. S.; Ding, J.; Vittal, J. J. Supramolecular Isomerism and Polyrotaxane-Based Two-Dimensional Coordination Polymers. *Cryst. Growth Des.* **2016**, *16*, 7278−7285.
(26) Hawes, C. S.; Knowles, G. P.; Chaffee, A. L.; Turner, D. R.; Batten, S. R. Modulating Porosity through Conformer-Dependent Hydrogen Bonding in Copper(II) Coordination Polymers. *Cryst. Growth Des.* **2015**, *15*, 3417−3425.
(27) Yang, X.-K.; Chen, J.-D. Crystal-to-crystal transformation and linker exchange in Cd(ii) coordination polymers based on flexible bis-pyridyl-bis-amide and 1,4-naphthalenedicarboxylate. *CrystEngComm* **2019**, *21*, 7437−7446.
(28) Notash, B.; Farhadi Rodbari, M.; Gallo, G.; Dinnebier, R. Humidity-Induced Structural Transformation in Pseudopolymorph Coordination Polymers. *Inorg. Chem.* **2021**, *60*, 9212−9223.
(29) Uemura, K. Syntheses and crystal structures of novel silver(I) coordination polymers based on linear or tetrahedral coordination environments. *Inorg. Chem. Commun.* **2008**, *11*, 741−744.
(30) Mendes, R. F.; Almeida Paz, F. A. Dynamic breathing effect in metal-organic frameworks: Reversible 2D-3D-2D-3D single-crystal to single-crystal transformation. *Inorg. Chim. Acta.* **2017**, *460*, 99−107.
(31) Santra, A.; Bharadwaj, P. K. Solvent-Induced Structural Diversity of Partially Fluorinated, Stable Pb(II) Metal-Organic Frameworks and Their Luminescence Properties. *Cryst. Growth Des.* **2014**, *14*, 1476−1485.
(32) Du, M.; Li, C.-P.; Wu, J.-M.; Guo, J.-H.; Wang, G.-C. Destruction and reconstruction of the robust $[Cu_2(OOCR)_4]$ unit during crystal structure transformations between two coordination polymers. *Chem. Commun.* **2011**, *47*, 8088−8090.
(33) Ke, S.-Y.; Wang, C.-C. Water-induced reversible SCSC or solid-state structural transformation in coordination polymers. *CrystEngComm* **2015**, *17*, 8776−8785.
(34) Liu, Z.-Y.; Yang, E.-C.; Li, L.-L.; Zhao, X.-J. A reversible SCSC transformation from a blue metamagnetic framework to a pink antiferromagnetic ordering layer exhibiting concomitant solvatochromic and solvatomagnetic effects. *Dalton Trans.* **2012**, *41*, 6827−6832.
(35) Zhuang, C.-F.; Zhang, J.; Wang, Q.; Chu, Z.-H.; Fenske, D.; Su, C.-Y. Temperature-Dependent Guest-Driven Single-Crystal-to-Single-Crystal Ligand Exchange in a Two-Fold Interpenetrated Cd^{II} Grid Network. *Chem.—Eur. J.* **2009**, *15*, 7578−7585.
(36) Zhang, X.-F.; Yan, T.; Wang, T.; Feng, J.; Wang, Q.; Wang, X.; Du, L.; Zhao, Q.-H. Single-crystal-to-single-crystal (SCSC) transformation and dissolution-recrystallization structural transformation (DRST) among three new copper(II) coordination polymers. *CrystEngComm* **2018**, *20*, 570−577.
(37) Sarma, D.; Natarajan, S. Usefulness of in Situ Single Crystal to Single Crystal Transformation (SCSC) Studies in Understanding the Temperature-Dependent Dimensionality Cross-over and Structural Reorganization in Copper-Containing Metal-Organic Frameworks (MOFs). *Cryst. Growth Des.* **2011**, *11*, 5415−5423.
(38) Karmakar, A.; Paul, A.; Pombeiro, A. J. L. Recent advances on supramolecular isomerism in metal organic frameworks. *CrystEngComm* **2017**, *19*, 4666−4695.
(39) Moulton, B.; Zaworotko, M. J. From Molecules to Crystal Engineering: Supramolecular Isomerism and Polymorphism in Network Solids. *Chem. Rev.* **2001**, *101*, 1629−1658.
(40) Schröder, M.; Champness, N. R. In *Encyclopedia of Supramolecular Chemistry*; Atwood, J. L., Steed, J. W., Eds.; Marcel Dekker: New York, 2004.
(41) Steed, J. W.; Atwood, J. L. *Supramolecular Chemistry*; John Wiley & Sons: Chichester, U.K., 2009.
(42) Hosseini, M. W. *Molecular Networks*; Springer: Germany, 2009.
(43) Miao, R.-Q.; Zhou, Q.-Q.; Wang, S.-Q.; Cheng, X.-Y.; Wang, D.-F.; Huang, R.-B. Solvent-induced Zn(II) coordination polymers with 1, 3, 5-benzenetricarboxylic acid. *J. Mol. Struct.* **2019**, *1184*, 219−224.
(44) Yao, J.; Chen, Q.; Sheng, Y.; Kai, A.; Liu, H. pH-controlled crystal growth of copper/gemini surfactant complexes with bipyridine groups. *CrystEngComm* **2017**, *19*, 5835−5843.
(45) Faust, T. B.; Usov, P. M.; D'Alessandro, D. M.; Kepert, C. J. Highly unusual interpenetration isomers of electroactive nickel bis(dithiolene) coordination frameworks. *Chem. Commun.* **2014**, *50*, 12772−12774.
(46) Sánchez-Férez, F.; Solans-Monfort, X.; Calvet, T.; Font-Bardia, M.; Pons, J. Controlling the Formation of Two Concomitant Polymorphs in Hg(II) Coordination Polymers. *Inorg. Chem.* **2022**, *61*, 4965−4979.
(47) Wang, C.-C.; Lin, W.-Z.; Huang, W.-T.; Ko, M.-J.; Lee, G.-H.; Ho, M.-L.; Lin, C.-W.; Shih, C.-W.; Chou, P.-T. New supramolecular isomers with 2D 4^4 square-grid and 3D $6^5{\cdot}8$ frameworks in a one-pot synthesis; reversible solvent uptake and intriguing luminescence properties. *Chem. Commun.* **2008**, 1299−1301.
(48) Nagarathinam, M.; Vittal, J. J. Anisotropic Movements of Coordination Polymers upon Desolvation: Solid-State Transformation of a Linear 1D Coordination Polymer to a Ladderlike Structure. *Angew. Chem., Int. Ed.* **2006**, *45*, 4337−4341.
(49) Nagarathinam, M.; Vittal, J. J. A Rational Approach to Crosslinking of Coordination Polymers Using the Photochemical [2+2] Cycloaddition Reaction. *Macromol. Rapid Commun.* **2006**, *27*, 1091−1099.
(50) Nagarathinam, M.; Vittal, J. J. Photochemical [2 + 2] cycloaddition as a tool to study a solid-state structural transformation. *Chem. Commun.* **2008**, 438−440.
(51) Kole, G. K.; Peedikakkal, A. M. P.; Toh, B. M. F.; Vittal, J. J. Solid-State Structural Transformations and Photoreactivity of 1D-Ladder Coordination Polymers of PbII. *Chem.—Eur. J.* **2013**, *19*, 3962−3968.

https://doi.org/10.1021/acsomega.3c00405
ACS Omega 2023, 8, 13140−13152

(52) Huang, C.; Zhu, K.; Zhang, Y.; Shao, Z.; Wang, D.; Mi, L.; Hou, H. Directed Structural Transformations of Coordination Polymers Supported Single-Site Cu(II) Catalysts To Control the Site Selectivity of C-H Halogenation. *Inorg. Chem.* **2019**, *58*, 12933−12942.
(53) Al-Mohsin, H. A.; AlMousa, A.; Oladepo, S. A.; Jalilov, A. S.; Fettouhi, M.; Peedikakkal, A. M. P. Single-Crystal-to-Single-Crystal Transformation of Hydrogen-Bonded Triple-Stranded Ladder Coordination Polymer via Photodimerization Reaction. *Inorg. Chem.* **2019**, *58*, 10167−10173.
(54) Lee, J. Y.; Lee, S. Y.; Sim, W.; Park, K.-M.; Kim, J.; Lee, S. S. Temperature-Dependent 3-D CuI Coordination Polymers of Calix[4]-bis-dithiacrown: Crystal-to-Crystal Transformation and Photoluminescence Change on Coordinated Solvent Removal. *J. Am. Chem. Soc.* **2008**, *130*, 6902−6903.
(55) Zhang, J.-P.; Lin, Y.-Y.; Zhang, W.-X.; Chen, X.-M. Temperature- or Guest-Induced Drastic Single-Crystal-to-Single-Crystal Transformations of a Nanoporous Coordination Polymer. *J. Am. Chem. Soc.* **2005**, *127*, 14162−14163.
(56) Maity, D. K.; Haque, F.; Halder, A.; Ghoshal, D. Reversible Switching of Frameworks through Single-Crystal-to-Single-Crystal Structural Transformation in Two Entangled Coordination Polymers and Their Impact on Adsorption Properties. *Cryst. Growth Des.* **2020**, *20*, 7667−7674.
(57) Cao, L.-H.; Li, H.-Y.; Xu, H.; Wei, Y.-L.; Zang, S.-Q. Diverse dissolution-recrystallization structural transformations and sequential Förster resonance energy transfer behavior of a luminescent porous Cd-MOF. *Dalton Trans.* **2017**, *46*, 11656−11663.
(58) Chen, J.-H.; Wei, D.; Yang, G.; Ma, J.-G.; Cheng, P. A systematic investigation of structural transformation in a copper pyrazolato system: a case study. *Dalton Trans.* **2020**, *49*, 1116−1123.
(59) Deng, Q.-J.; Chen, M.; Chen, D.-C.; Long, H.-Y.; Chen, C.-A. Tracking the dissolution-recrystallization structural transformation (DRST) of copper(II) complexes: a combined crystallographic, mass spectrometric and DFT study. *Acta Crystallogr., Sect. C: Cryst. Struct. Commun.* **2020**, *76*, 655−662.
(60) Ejarque, D.; Calvet, T.; Font-Bardia, M.; Pons, J. Amide-Driven Secondary Building Unit Structural Transformations between Zn(II) Coordination Polymers. *Cryst. Growth Des.* **2022**, *22*, 5012−5026.
(61) Ciurtin, D. M.; Dong, Y.-B.; Smith, M. D.; Barclay, T.; zur Loye, H.-C. Two Versatile N,N'-Bipyridine-Type Ligands for Preparing Organic−Inorganic Coordination Polymers: New Cobalt- and Nickel-Containing Framework Materials. *Inorg. Chem.* **2001**, *40*, 2825−2834.
(62) Lozovan, V.; Coropceanu, E. B.; Bourosh, P. N.; Micu, A.; Fonari, M. S. Coordination Polymers of Zn and Cd Based on Two Isomeric Azine Ligands: Synthesis, Crystal Structures, and Luminescence Properties. *Russ. J. Coord. Chem.* **2019**, *45*, 11−21.
(63) Spek, A. L. PLATON SQUEEZE: a tool for the calculation of the disordered solvent contribution to the calculated structure factors. *Acta Crystallogr., Sect. C: Cryst. Struct. Commun.* **2015**, *C71*, 9−18.
(64) Rachuri, Y.; Parmar, B.; Bisht, K. K.; Suresh, E. Solvothermal self-assembly of Cd^{2+} coordination polymers with supramolecular networks involving N-donor ligands and aromatic dicarboxylates: synthesis, crystal structure and photoluminescence studies. *Dalton Trans.* **2017**, *46*, 3623−3630.
(65) Zhang, G.; Yang, G.; Ma, J. S. Anion Control of the Self-Assembly of One-Dimensional Molecular Ladders vs Three-Dimensional Cross-like Arrays Based on a Bidentate Schiff Base Ligand. *Cryst. Growth Des.* **2006**, *6*, 1897−1902.
(66) Nagarathinam, M.; Chanthapally, A.; Lapidus, S. H.; Stephens, P. W.; Vittal, J. J. Mechanochemical reactions of coordination polymers by grinding with KBr. *Chem. Commun.* **2012**, *48*, 2585−2587.
(67) Janiak, C. A critical account on $\pi-\pi$ stacking in metal complexes with aromatic nitrogen-containing ligands. *Dalton Trans.* **2000**, 3885−3896.
(68) Blatov, V. A. Multipurpose Crystallochemical Analysis with the program package TOPOS. *IUCr CompComm Newsletter* **2006**, *7*, 4.
(69) Edgington, P. R.; McCabe, P.; Macrae, C. F.; Pidcock, E.; Shields, G. P.; Taylor, R.; Towler, M.; Van De Streek, J. Mercury: visualization and analysis of crystal structures. *J. Appl. Crystallogr.* **2006**, *39*, 453−457.
(70) Ohtsu, H.; Kawano, M. Kinetic assembly of coordination networks. *Chem. Commun.* **2017**, *53*, 8818−8829.
(71) Zhang, J.; Wojtas, L.; Larsen, R. W.; Eddaoudi, M.; Zaworotko, M. J. Temperature and Concentration Control over Interpenetration in a Metal−Organic Material. *J. Am. Chem. Soc.* **2009**, *131*, 17040−17041.
(72) Forster, P. M.; Burbank, A. R.; Livage, C.; Férey, G.; Cheetham, A. K. The role of temperature in the synthesis of hybrid inorganic-organic materials: the example of cobalt succinates. *Chem. Commun.* **2004**, 368−369.
(73) Werner, J.; Rams, M.; Tomkowicz, Z.; Runčevski, T.; Dinnebier, R. E.; Suckert, S.; Näther, C. Thermodynamically Metastable Thiocyanato Coordination Polymer That Shows Slow Relaxations of the Magnetization. *Inorg. Chem.* **2015**, *54*, 2893−2901.
(74) Nagarkar, S. S.; Chaudhari, A. K.; Ghosh, S. K. Role of Temperature on Framework Dimensionality: Supramolecular Isomers of $Zn_3(RCOO)_8$ Based Metal Organic Frameworks. *Cryst. Growth Des.* **2012**, *12*, 572−576.
(75) Pavia, D.; Lampman, G.; Kriz, G. *Introduction to spectroscopy*; Thomason learning: U. S. A, 2001.
(76) Nakamoto, K. *Infrared and Raman Spectra of Inorganic and Coordination Compounds Part B:Applications in Coordination, Organometallic, and Bioinorganic Chemistry*; John Wiley & Sons: Chichester, U.K., 2009.

https://doi.org/10.1021/acsomega.3c00405
ACS Omega 2023, 8, 13140−13152